Data-based determination of the isospin-limit light-quark-connected contribution to the anomalous magnetic moment of the muon

Diogo Boito,[1] Maarten Golterman,[2,3] Kim Maltman,[4,5] and Santiago Peris[3]

[1]*Instituto de Física de São Carlos, Universidade de São Paulo CP 369, 13570-970, São Carlos, São Paulo, Brazil*

[2]*Department of Physics and Astronomy, San Francisco State University, San Francisco, California 94132, USA*

[3]*Department of Physics and IFAE-BIST, Universitat Autònoma de Barcelona E-08193 Bellaterra, Barcelona, Spain*

[4]*Department of Mathematics and Statistics, York University Toronto, Ontario, Canada M3J 1P3*

[5]*CSSM, University of Adelaide, Adelaide, South Australia 5005 Australia*

(Received 2 December 2022; accepted 13 March 2023; published 3 April 2023)

We describe how recent determinations of exclusive-mode contributions to $a_\mu^{\mathrm{LO,HVP}}$, the leading-order hadronic vacuum polarization contribution to the anomalous magnetic moment of the muon, can be used to provide, up to small electromagnetic (EM) corrections accessible from the lattice, a data-based dispersive determination of $a_\mu^{\mathrm{lqc;IL}}$, the isospin-limit, light-quark-connected contribution to $a_\mu^{\mathrm{LO,HVP}}$. Such a determination is of interest in view of the existence of a number of lattice results for this quantity, emerging evidence for a tension between lattice and dispersive determinations of $a_\mu^{\mathrm{LO,HVP}}$, and the desire to clarify the source of this tension. Taking as input for the small EM correction that must be applied to the purely data-driven dispersive determination the result $-0.93(58) \times 10^{-10}$ obtained in a recent BMW lattice study, we find $a_\mu^{\mathrm{lqc;IL}}$ to be $635.0(2.7) \times 10^{-10}$ if the results of Keshavarzi, Nomura, and Teubner are used for the exclusive-mode contributions and $638.4(4.1) \times 10^{-10}$ if instead those of Davier, Höcker, Malaescu, and Zhang are used.

DOI: 10.1103/PhysRevD.107.074001

I. INTRODUCTION

As is well known, the recent FNAL E989 result [1] for the anomalous magnetic moment of the muon, $a_\mu = (g-2)/2$, is in good agreement with the earlier BNL E821 result [2], producing an updated world average which is 4.2σ larger than the Standard Model (SM) expectation detailed in the $g-2$ theory initiative assessment [3], and based on the work of Refs. [4–27].

In determining SM contributions to a_μ, a particularly important role is played by the leading-order, hadronic vacuum polarization contribution, $a_\mu^{\mathrm{LO,HVP}}$, the uncertainty on which dominates that on the SM expectation for a_μ. The assessment of $a_\mu^{\mathrm{LO,HVP}}$ arrived at in Ref. [3] is based on the results of two analyses [10,11] using the standard dispersive representation [28–30] with current $e^+e^- \to$ hadrons cross-section data as input, supplemented by additional input from Refs. [12,13] for $\pi\pi$ contributions below 1 GeV^2 and 3π contributions. The SM expectation for $a_\mu^{\mathrm{LO,HVP}}$ can, however, also be obtained on the lattice using the alternate, weighted Euclidean integral representation [31–33] and there has been intense recent activity in the lattice community aimed at reducing lattice errors to a level sufficient to make lattice results competitive with the dispersive determination [34–61]. The most recent lattice result from the BMW collaboration [50] comes close to this goal, reaching, for the first time, subpercent precision. This result, however, is in tension with the dispersive value for $a_\mu^{\mathrm{LO,HVP}}$. This tension is also seen, at an enhanced (up to 3.9σ) level, in comparisons of dispersive [50,62] and lattice [48,50,51,55–58,60,61] results for the intermediate window quantity, a_μ^W, introduced by the RBC/UKQCD collaboration [40]. Similar tensions, reaching as much as 3.7σ, are also found for the one-sided windows considered in Ref. [59].

Lattice results for $a_\mu^{\mathrm{LO,HVP}}$ are typically quoted as sums of isospin-limit light-, strange-, charm-, and bottom-quark connected contributions, the disconnected contribution,

Published by the American Physical Society under the terms of the Creative Commons Attribution 4.0 International license. Further distribution of this work must maintain attribution to the author(s) and the published article's title, journal citation, and DOI. Funded by SCOAP³.

and strong-isospin-breaking (SIB) and electromagnetic (EM) contributions, the latter two receiving both connected and disconnected contributions. By far the largest of these contributions is the isospin-limit light-quark-connected one, denoted $a_\mu^{\rm lqc;IL}$ in what follows. Although continuum/dispersive estimates exist for the SIB contribution [63,64], and, from our recent work [65], for the sum of the strange-quark-connected and full disconnected contributions, no dispersive result exists for $a_\mu^{\rm lqc;IL}$. In this paper, we remedy this situation, performing an almost-completely data-based determination of $a_\mu^{\rm lqc;IL}$. Our result confirms the existence of a tension between the dispersive determination and the most precise of the lattice determinations [50]. We also indicate how the same analysis strategy can, in principle, be employed to obtain isospin-limit, light-quark-connected contributions to analogous reweighted/window observables such as the RBC/UKQCD intermediate window quantity, $a_\mu^{\rm W}$ [40], the one-sided window quantities of Ref. [59], and the window quantities of Ref. [66], based on s-dependent weights designed to produce results for the associated dispersive determinations focused on more limited regions in s. Work on the reweighted exclusive-mode integrals needed to complete such analyses is in progress, and will be reported on elsewhere. In the present paper we focus on the quantity $a_\mu^{\rm lqc;IL}$, where existing results for exclusive-mode contributions to $a_\mu^{\rm LO,HVP}$ already make a dispersive determination possible.

The rest of the paper is organized as follows. In Sec. II we detail how, in the isospin limit, dispersive results for the exclusive-mode contributions to $a_\mu^{\rm LO,HVP}$ can be used to provide a dispersive determination of $a_\mu^{\rm lqc;IL}$. In Sec. III we implement this analysis, ignoring for the moment isospin-breaking (IB) corrections, using as input for the exclusive-mode contributions those determined in Refs. [10,11]. In Sec. IV, we discuss (and evaluate) IB corrections to the results obtained in Sec. III. This section also contains our final results for $a_\mu^{\rm lqc;IL}$. Finally, in Sec. V we provide a brief summary and discuss how, using more detailed exclusive-mode information, in the form of the s-dependence of exclusive-mode contributions to the R-ratio, $R(s)$, analogous results for the isospin-limit, light-quark-connected contributions to differently weighted integrals over $R(s)$, such as the window quantities noted above, can also be obtained.

II. BASIC ANALYSIS STRATEGY

A. Notation

We begin with some basic notation and associated isospin decompositions.

Key objects in the analysis are the two-point functions, $\Pi^{ab}_{\mu\nu}(q)$, of the flavor-octet, vector currents $V^a_\mu = \bar q \frac{\lambda^a}{2}\gamma_\mu q$, $a = 1, \cdots 8$, (where λ^a are the usual Gell-Mann matrices) together with the associated polarizations, $\Pi^{ab}(Q^2)$, subtracted polarizations, $\hat\Pi^{ab}(Q^2)$, and spectral functions, $\rho^{ab}(s)$, defined by

$$\begin{aligned}\Pi^{ab}_{\mu\nu}(q) &= (q_\mu q_\nu - q^2 g_{\mu\nu})\Pi^{ab}(Q^2) \\ &= i\int d^4x e^{iq\cdot x}\langle 0|T(V^a_\mu(x)V^b_\nu(0))|0\rangle, \end{aligned} \tag{2.1}$$

$$\hat\Pi^{ab}(Q^2) = \Pi^{ab}(Q^2) - \Pi^{ab}(0), \tag{2.2}$$

$$\rho^{ab}(s) = \frac{1}{\pi}{\rm Im}\Pi^{ab}(Q^2), \quad (s = -Q^2 > 0), \tag{2.3}$$

where $s = q^2$ and $Q^2 = -q^2$.

The decomposition of the u, d, s part of the EM current, $J^{\rm EM}_\mu$, into isovector ($a = 3$) and isoscalar ($a = 8$) parts,

$$J^{\rm EM}_\mu = V^3_\mu + \frac{1}{\sqrt{3}}V^8_\mu \equiv J^{\rm EM,3}_\mu + J^{\rm EM,8}_\mu, \tag{2.4}$$

leads to the following decompositions for the subtracted three-flavor EM vacuum polarization, $\hat\Pi_{\rm EM}(Q^2)$, and spectral function, $\rho_{\rm EM}(s)$,

$$\begin{aligned}\hat\Pi_{\rm EM}(Q^2) &= \hat\Pi^{33}_{\rm EM}(Q^2) + \frac{2}{\sqrt{3}}\hat\Pi^{38}_{\rm EM}(Q^2) + \frac{1}{3}\hat\Pi^{88}_{\rm EM}(Q^2) \\ &\equiv \hat\Pi^{I=1}_{\rm EM}(Q^2) + \hat\Pi^{\rm MI}_{\rm EM}(Q^2) + \hat\Pi^{I=0}_{\rm EM}(Q^2), \\ \rho_{\rm EM}(s) &= \rho^{33}(s) + \frac{2}{\sqrt{3}}\rho^{38}(s) + \frac{1}{3}\rho^{88}(s) \\ &\equiv \rho^{I=1}_{\rm EM}(s) + \rho^{\rm MI}_{\rm EM}(s) + \rho^{I=0}_{\rm EM}(s), \end{aligned} \tag{2.5}$$

with the $ab = 33$ parts pure isovector, the $ab = 88$ parts pure isoscalar and the $ab = 38$ parts mixed isospin terms which vanish in the isospin limit. In the isospin limit $\hat\Pi^{33}$ is pure light-quark-connected while $\hat\Pi^{88}$ contains light-quark-connected, strange-quark-connected and all disconnected contributions.

The leading-order hadronic contribution to a_μ, $a_\mu^{\rm LO,HVP}$, is related to $R(s) = 12\pi^2\rho_{\rm EM}(s)$ by the standard "dispersive" representation [28–30],

$$a_\mu^{\rm LO,HVP} = \frac{\alpha^2_{\rm EM}m^2_\mu}{9\pi^2}\int_{m^2_\pi}^\infty ds\frac{\hat K(s)}{s^2}R(s), \tag{2.6}$$

with $\alpha_{\rm EM}$ the EM fine-structure constant, $R(s)$ determined from the bare inclusive hadronic electroproduction cross section, $\sigma^{(0)}[e^+e^- \to hadrons(+\gamma)]$, by

$$R(s) = \frac{3s}{4\pi\alpha^2_{\rm EM}}\sigma^{(0)}[e^+e^- \to hadrons(+\gamma)], \tag{2.7}$$

and the kernel $\hat K(s)$ an exactly known, slowly (and monotonically) increasing function of s (see, e.g., Ref. [3]).

Dispersive determinations of $a_\mu^{\rm LO,HVP}$ are typically obtained by summing (i) exclusive-mode contributions up to just below $s = 4\ {\rm GeV}^2$, (ii) narrow charm and bottom resonance contributions, and (iii) contributions evaluated using inclusive $R(s)$ data and/or perturbative QCD (pQCD) in the remainder of the high-s region. The exclusive-mode regions in the analyses of Refs. [10,11] we employ below are $s \le (1.8\ {\rm GeV})^2 = 3.24\ {\rm GeV}^2$ and $s \le (1.937\ {\rm GeV})^2 = 3.7520\ {\rm GeV}^2$, respectively.

The isospin decomposition of $\hat\Pi_{\rm EM}$ in Eq. (2.5) leads to the related decomposition for the three-flavor (u, d, s) contribution to $a_\mu^{\rm LO,HVP}$,

$$a_\mu^{\rm LO,HVP} = a_\mu^{33} + \frac{2}{\sqrt{3}} a_\mu^{38} + \frac{1}{3} a_\mu^{88} \equiv a_\mu^{I=1} + a_\mu^{\rm MI} + a_\mu^{I=0}. \tag{2.8}$$

To first order in $m_d - m_u$ there are no SIB contributions to either a_μ^{33} or a_μ^{88}, while SIB is expected to dominate a_μ^{38}.

In what follows, we will also denote contributions from an individual exclusive mode, X, to $a_\mu^{\rm LO,HVP}$, $a_\mu^{I=1}$, $a_\mu^{I=0}$ and $a_\mu^{\rm MI}$ by $[a_\mu^{\rm LO,HVP}]_X$, $[a_\mu^{I=1}]_X$, $[a_\mu^{I=0}]_X$, and $[a_\mu^{\rm MI}]_X$, respectively.

B. The basic idea

The basic idea underlying the analysis is as follows. In the isospin limit, $\hat\Pi_{\rm EM}^{I=1}$ is pure light-quark-connected, while $\hat\Pi_{\rm EM}^{I=0}$ is a sum of light-quark-connected, strange-quark-connected and all disconnected contributions, with light-quark-connected contribution

$$[\hat\Pi_{\rm EM}^{I=0}]^{\rm lqc} = \frac{1}{9}\hat\Pi_{\rm EM}^{I=1}. \tag{2.9}$$

The full light-quark-connected contribution to $\hat\Pi_{\rm EM}$ is thus

$$\hat\Pi_{\rm EM}^{\rm lqc} \equiv \frac{10}{9}\hat\Pi_{\rm EM}^{I=1} \tag{2.10}$$

and the corresponding spectral function

$$\rho_{\rm EM}^{\rm lqc}(s) = \frac{10}{9}\rho_{\rm EM}^{I=1}(s). \tag{2.11}$$

The desired light-quark-connected contribution to $a_\mu^{\rm LO,HVP}$, $a_\mu^{\rm lqc;IL}$, is then given by the following dispersive integral involving the $I = 1$ spectral function:

$$a_\mu^{\rm lqc,IL} = \frac{\alpha_{\rm EM}^2 m_\mu^2}{9\pi^2}\int_{m_\pi^2}^\infty ds \frac{\hat K(s)}{s^2}\left[\left(\frac{10}{9}\right)12\pi^2\rho_{\rm EM}^{I=1}(s)\right]. \tag{2.12}$$

An accurate determination of $a_\mu^{\rm lqc;IL}$ is thus possible provided the $I = 1$ contribution to $R(s)$, or equivalently $\rho_{\rm EM}(s)$, can be identified with sufficient precision.

The separation of $I = 1$ and $I = 0$ contributions is straightforward in the higher-s inclusive region, where $R(s)$ is approximated using pQCD and the $I = 1$ part represents 3/4 of the total. In the lower-s region, where $R(s)$ is obtained as a sum over exclusive-mode contributions, the separation is also straightforward for those exclusive modes having well-defined G-parity since states with positive/negative G-parity necessarily have $I = 1/I = 0$. This provides unique isospin assignments for contributions from exclusive modes consisting entirely of narrow and/or strong-interaction-stable states having well-defined G-parity (π, η, ω, ϕ), which constitute more than 93% of the total exclusive-mode-region contribution. Further input is needed to separate the $I = 1$ and $I = 0$ components of contributions from exclusive modes which are not eigenstates of G-parity, such as those containing at least one $K\bar K$ pair. We outline in the next section how this separation is accomplished using experimental input for the $K\bar K$ and $K\bar K\pi$ exclusive modes. For all other G-parity-ambiguous exclusive modes, X, we employ a "maximally conservative" assessment in which the $I = 1$ contribution, $[a_\mu^{I=1}]_X$, is taken to be $50 \pm 50\%$ of the total $[a_\mu^{\rm LO,HVP}]_X$. Fortunately, spectral contributions from these additional G-parity-ambiguous modes lie at higher s and thus have contributions to $a_\mu^{\rm LO,HVP}$, and hence also $I = 0/1$ separation uncertainties, which are strongly numerically suppressed, in spite of their 100% uncertainties.

In Sec. III we will implement the above analysis framework using as input the exclusive-mode results of Refs. [10,11], neglecting, to begin with, isospin-breaking (IB) corrections. The resulting nominal $a_\mu^{\rm lqc;IL}$, which we will denote by $a_\mu^{\rm lqc}$, will differ from the desired isospin-limit value by small IB contributions. These IB contributions are taken into account and removed in Sec. IV, which contains our final results for $a_\mu^{\rm lqc;IL}$.

III. A DATA-BASED IMPLEMENTATION IGNORING ISOSPIN-BREAKING EFFECTS

In this section we carry out two determinations of $a_\mu^{\rm lqc}$, neglecting IB corrections. These differ in the input used for the exclusive-mode $a_\mu^{\rm LO,HVP}$ contributions, one employing the results of Ref. [11] (KNT19), the other those of Ref. [10] (DHMZ). The reader is reminded that the KNT19 and DHMZ exclusive-mode regions are different, the former extending up to $s = 3.7520\ {\rm GeV}^2$, the latter up to only $s = 3.24\ {\rm GeV}^2$. Contributions from the region above these exclusive-mode endpoints will be obtained using pQCD,[1] with an error component, to be discussed below, designed to

[1]The shorthand "pQCD" refers here, and in what follows, to dimension $D = 0$, mass-independent perturbative OPE contributions. For the $I = 1$ polarization $\Pi_{\rm EM}^{I=1}$ considered this paper, mass-dependent $D = 2$ perturbative corrections are $O(m_{u,d}^2)$, and numerically negligible.

take into account possible small duality-violating (DV) contributions. The higher onset in s of the inclusive region for KNT19 increases the expected accuracy of the pQCD result used to represent $\rho_{\rm EM}^{I=1}(s)$ in this region and constitutes an advantage for the determination employing KNT19 input over that employing DHMZ input. Details of the form of the pQCD representation used in the inclusive region, together with our strategy for estimating possible residual DV corrections, are provided in Sec. III A.

The KNT19- and DHMZ-based analyses are outlined in Sec. III B below. In both cases we take advantage of results already worked out in Ref. [65]. This includes results for the data-based $I = 0/1$ separation of $K\bar{K}$ and $K\bar{K}\pi$ contributions. For the reader's benefit, the paragraphs which follow briefly review the treatment of the contributions from these modes. Further details may be found in Secs. IV.B and IV.C of Ref. [65].

$K\bar{K}$ contributions to $a_\mu^{\rm LO,HVP}$ are expected to be dominated by the $I = 0$ contribution of the ϕ resonance, with a much smaller $I = 1$ contribution. This qualitative expectation can be quantified by combining the electroproduction-based result for the sum of $I = 1$ and 0 contributions with recent *BABAR* results [67] for the differential $\tau^- \to K^- K^0 \nu_\tau$ decay distribution, which provides an experimental determination of the charged $I = 1$ vector current spectral function, and, via the conserved vector current (CVC) relation, up to numerically negligible IB corrections, an experimental determination of the $I = 1$ $K\bar{K}$-mode contribution to $\rho_{\rm EM}(s)$. In the region where it is rather precise (up to $s = 2.7556\ {\rm GeV}^2$, well above the ϕ peak), the *BABAR* τ data can thus be used to provide a direct determination of the $I = 1$ $K\bar{K}$ contribution to $a_\mu^{\rm LO,HVP}$. For the contributions from the parts of the KNT19 and DHMZ exclusive-mode regions above $2.7556\ {\rm GeV}^2$, we employ the maximally conservative separation treatment of KNT19 results for the $K\bar{K}$ contributions to $R(s)$. The contributions from this region turn out to be much smaller than those from the region covered by the *BABAR* τ data. Note that KNT19 $K\bar{K}$ input is used for the determination of this higher-s $K\bar{K}$ exclusive-mode contribution for both the KNT19- and DHMZ-based versions of the analyses. The reason is that the full $K\bar{K}$ exclusive-mode data and covariances are publicly available only in the KNT19 case. Numerical details for the KNT19- and DHMZ-based analyses are provided below.

The exclusive-mode-region, $I = 1$, $K\bar{K}\pi$-mode contributions to $a_\mu^{\rm LO,HVP}$ are obtained using the Dalitz-plot-based $I = 1/0$ separation of $K\bar{K}\pi$ cross-sections performed by *BABAR* [68], an analysis made possible by the observed saturation of the cross sections in the region of interest for this paper by KK^* contributions.

A. pQCD and DV corrections in the inclusive region

For the pQCD expression used to represent $\rho_{\rm EM}^{I=1}(s)$ in the inclusive region, we employ the standard five-loop, $n_f = 3$ pQCD result [69,70] with PDG2020 input for α_s [71]. $D = 2$, perturbative quark-mass-squared corrections are completely negligible. In the region from just below $\sqrt{s} = 2$ GeV up to charm threshold, $n_f = 3$ perturbative expectations for $R(s)$ are compatible within errors with the experimental determinations of BES [72,73] and KEDR [74] (especially those of KEDR [74]), but lie slightly below recent BESIII results [75]. Small residual DV contributions to $\rho_{\rm EM}(s)$ may thus be present even in this relatively large-s region, making it important to estimate the impact of possible DV corrections to $\rho_{\rm EM}^{I=1}(s)$ in the inclusive region of our analyses as well. While the whole of the KNT19 inclusive region lies in the region of agreement with BES and KEDR, the lower part of the DHMZ inclusive region extends to lower s, where the deviation of the perturbative expectation for $R(s)$ from the experimental sum-of-exclusive-mode-contributions determination is larger. An estimate of possible DV corrections to the pQCD approximation is thus of even more importance for the DHMZ-based analysis.

We investigate possible DV corrections using recent results for DV contributions to the charged $I = 1$ vector current spectral function, $\rho_{\rm ud;V}(s)$, measured in hadronic τ decays. $\rho_{\rm ud;V}(s)$ is related to the conventionally normalized EM isovector spectral function, $\rho_{\rm EM}^{I=1}(s)$ by the CVC relation, $\rho_{\rm EM}^{I=1}(s) = \frac{1}{2}\rho_{\rm ud;V}(s)$. In Ref. [76], finite-energy sum rule (FESR) analyses of weighted integrals of a recently improved version of $\rho_{\rm ud;V}(s)$ were carried out using the large-s ansatz

$$[\rho_{\rm ud;V}]_{\rm DV}(s) = \exp(-\delta_1 - \gamma_1 s)\sin(\alpha_1 + \beta_1 s), \qquad (3.1)$$

for the DV contribution to $\rho_{ud;V}(s)$. As detailed in Ref. [77], this ansatz follows for massless quarks from large-N_c and Regge arguments. The DV parameters δ_1, γ_1, α_1, and β_1, were obtained as part of the FESR fits. A range of different fits was considered, characterized by the choice of $s_{\rm min}$, the minimum s for which the DV ansatz was to be employed. Of these, ten, with $s_{\rm min}$ lying between 1.4251 and $1.7256\ {\rm GeV}^2$, show excellent p-values, good stability of the DV parameter results between the different fits, and reasonably controlled DV parameter errors. With all these $s_{\rm min}$ lying below the onset of both the KNT19 and DHMZ inclusive regions, it is thus possible to consider integrated DV contributions to $a_\mu^{\rm lqc}$ in the inclusive region using any of these fits. We evaluate the DV contributions and associated errors for each of these fits. We then take as the central value of our estimate of the DV contribution the midpoint of the range spanned by these results and their errors, and as the uncertainty on that estimate half of that range. Numerical details for the KNT19 and DHMZ cases are provided below.

B. $a_\mu^{\rm lqc}$ using KNT19 or DHMZ exclusive-mode input

We now turn to KNT19- and DHMZ-based determinations of $a_\mu^{\rm lqc}$, neglecting small IB corrections, which will be dealt with in the next section.

We begin with the KNT19-based analysis. Reference [65] provides the following results for the various KNT19-based contributions to $a_\mu^{I=1}$.

The sum of all KNT19 G-parity-positive exclusive-mode contributions to $a_\mu^{\rm LO,HVP}$ from the region $s \le 3.7520\ {\rm GeV}^2$ is

$$[a_\mu^{I=1}]_{G=+} = 543.21(2.09) \times 10^{-10}. \tag{3.2}$$

The breakdown, showing the modes which contribute and the KNT19 contribution from each, may be found in Table I of Ref. [65].

The $I = 1$ part of the G-parity-ambiguous $K\bar{K}$ contribution from threshold to $3.7520\ {\rm GeV}^2$ is

$$[a_\mu^{I=1}]_{K\bar{K}} = 0.85(9) \times 10^{-10}. \tag{3.3}$$

The $I = 1$ part of the G-parity-ambiguous $K\bar{K}\pi$ contribution from threshold to $3.7520\ {\rm GeV}^2$ is

$$[a_\mu^{I=1}]_{K\bar{K}\pi} = 0.74(12) \times 10^{-10}. \tag{3.4}$$

The $I = 1$ $K\bar{K}2\pi$ mode contribution is obtained by first subtracting from the KNT19 $I = 1 + 0$ total, $[a_\mu^{\rm LO,HVP}]_{K\bar{K}2\pi} = 1.93(8) \times 10^{-10}$, the purely $I = 0$ component, $0.159(10) \times 10^{-10}$, resulting from $e^+e^- \to \phi\pi\pi$ with the ϕ subsequently decaying to $K\bar{K}$, and then applying the maximally conservative $50 \pm 50\%$ assessment of the $I = 1$ contribution to the resulting still-ambiguous difference. The result is

$$[a_\mu^{I=1}]_{K\bar{K}2\pi} = 0.89(89) \times 10^{-10}. \tag{3.5}$$

The $I = 0$ $\phi\pi\pi$ subtraction was evaluated using the $e^+e^- \to \phi\pi\pi$ cross sections reported in Ref. [78].

The sum of the total $(I = 1 + 0)$ contributions to $a_\mu^{\rm LO,HVP}$ from all remaining G-parity ambiguous KNT19 modes, as detailed in the Appendix of Ref. [65], is $0.23(3) \times 10^{-10}$, leading to a maximally conservative estimate of the corresponding $I = 1$ contribution

$$[a_\mu^{I=1}]_{\rm other} = 0.12(12) \times 10^{-10}. \tag{3.6}$$

The KNT19 inclusive region $I = 1$ pQCD contribution is a factor $9/2$ times the corresponding strange-connected-plus-disconnected contribution reported in Ref. [65], and hence

$$[a_\mu^{I=1}]_{\rm pQCD} = 28.27(2) \times 10^{-10}. \tag{3.7}$$

The uncertainty reflects that on the input value of α_s and the estimated impact of 5-loop truncation and is much smaller than the size of the estimated DV contribution, obtained as discussed above,[2]

$$[a_\mu^{I=1}]_{\rm DV} = 0.26(12) \times 10^{-10}. \tag{3.8}$$

The total KNT19 inclusive region contribution, including this estimate of the DV correction, is thus

$$[a_\mu^{I=1}]_{\rm incl} = 28.53(26) \times 10^{-10}, \tag{3.9}$$

where, to be conservative, we have assigned the full central value of the estimated DV correction as an expanded uncertainty.

Adding the above contributions yields the following interim result, prior to applying IB corrections, for the $I = 1$ contribution

$$a_\mu^{I=1} = 574.34(2.29) \times 10^{-10} \tag{3.10}$$

and hence the associated interim light-quark-connected result

$$a_\mu^{\rm lqc} = 638.16(2.55) \times 10^{-10}. \tag{3.11}$$

Turning now to the analogous DHMZ-based analysis, once more relying heavily on results already detailed in Ref. [65], we find the following results for the components of the DHMZ-based determination of $a_\mu^{I=1}$.

The sum of all DHMZ G-parity positive exclusive-mode contributions to $a_\mu^{\rm LO,HVP}$ from the region $s \le 3.24\ {\rm GeV}^2$ is

$$[a_\mu^{I=1}]_{G=+} = 542.74(3.39)(1.12)_{\rm lin} \times 10^{-10}, \tag{3.12}$$

where the first error is the quadrature sum of the statistical and mode-specific, mode-to-mode-uncorrelated systematic errors of Ref. [10], and the second is the 100%-correlated common systematic error. The subscript "lin" is a reminder of the fact that, as specified in Ref. [10], this error is obtained by summing linearly the corresponding errors on the individual DHMZ exclusive-mode contributions.

The DHMZ contributions from G-parity-ambiguous exclusive modes in the region $s \le 3.24\ {\rm GeV}^2$ are

$$[a_\mu^{I=1}]_{K\bar{K}} = 0.83(8) \times 10^{-10}, \tag{3.13}$$

$$[a_\mu^{I=1}]_{K\bar{K}\pi} = 0.66(11) \times 10^{-10}, \tag{3.14}$$

$$[a_\mu^{I=1}]_{K\bar{K}2\pi} = 0.37(37) \times 10^{-10}. \tag{3.15}$$

[2]The DV contributions to $a_\mu^{I=1}$ obtained from the ten fits noted above lie between $0.21(8) \times 10^{-10}$ and $0.26(12) \times 10^{-10}$, and hence cover the range from 0.13×10^{-10} to 0.38×10^{-10}. The central value and error of the result quoted in Eq. (3.8) represent, respectively, the midpoint and half the extent of this range.

$$[a_\mu^{I=1}]_{\text{other}} = 0.00(1) \times 10^{-10}, \tag{3.16}$$

with all results, with the exception of that from the $K\bar{K}2\pi$ mode, given previously in Sec. VI of Ref. [65]. The additional information needed to obtain the $K\bar{K}2\pi$ result is as follows. First, the DHMZ result for the total $I = 1 + 0$ contribution to $a_\mu^{\text{LO,HVP}}$ is $0.85(2)(5)(1)_{\text{lin}} \times 10^{-10}$. Second, the $s \leq 3.24$ GeV^2, $I = 0$ $\phi(\to K\bar{K})\pi\pi$ contribution implied by *BABAR* $e^+e^- \to \phi\pi\pi$ cross-sections [78] is $0.117(8) \times 10^{-10}$. The G-parity ambiguous $K\bar{K}2\pi$ remainder is thus $0.73(5)(1)_{\text{lin}} \times 10^{-10}$ and the maximally conservative assessment of the $I = 1$ component thereof $0.37(37) \times 10^{-10}$, where we have ignored all error components other than the strongly dominant maximally conservative separation uncertainty.

Finally, for the DHMZ inclusive region pQCD, DV and total contributions, we find

$$[a_\mu^{I=1}]_{\text{pQCD}} = 32.74(3) \times 10^{-10}, \tag{3.17}$$

$$[a_\mu^{I=1}]_{\text{DV}} = -0.19(31) \times 10^{-10}, \tag{3.18}$$

$$[a_\mu^{I=1}]_{\text{incl}} = 32.55(31) \times 10^{-10}. \tag{3.19}$$

We note that the uncertainty on the DV contribution in this case is significantly larger than that obtained for the KNT19 case above.[3]

Adding the above contributions yields the following interim DHMZ-based result

$$a_\mu^{I=1} = 577.15(3.43)(1.12)_{\text{lin}} \times 10^{-10} \tag{3.20}$$

and hence the associated interim light-quark-connected result

$$a_\mu^{\text{lqc}} = 641.28(3.81)(1.24)_{\text{lin}} \times 10^{-10}. \tag{3.21}$$

The final step required to obtain the desired isospin-limit version, $a_\mu^{\text{lqc;IL}}$, of a_μ^{lqc} is to apply EM and SIB corrections to the interim results (3.11) and (3.21). This step is discussed in the next section.

IV. EM AND SIB CORRECTIONS

In this section we consider EM and SIB corrections to the results above. In assessing EM corrections, we will take advantage of the results of the recent BMW lattice study [50], which provides the first determination of all EM $a_\mu^{\text{LO,HVP}}$ contributions on the lattice. We consider use of the lattice determination unavoidable at present since, while a number of contributions to the total EM correction can be reliably estimated using dispersive/data-driven approaches (see, e.g., Ref. [79]), there are other, potentially non-negligible contributions for which no reliable methods of obtaining a data-driven estimate are currently known. The existence of strong cancellations in the sum of currently known contributions [79], moreover, enhances the potential numerical importance of such yet-to-be-evaluated contributions. An example of such a potentially important "missing" contribution is the EM component of the ρ-region $\pi\pi$ contribution to $a_\mu^{\text{LO,HVP}}$. EM effects will be present at some level in the physical ρ^0 decay constant, the $\rho\pi\pi$ coupling, the ρ^0 width and even the ρ^0 mass [80]. Given the failure, to date, of attempts to reproduce the observed difference between EM and τ-decay-based determinations of the ρ-region $\pi\pi$ contribution to the $I = 1$ vector current spectral function,[4] it is clear that no reliable data-driven method is currently available for estimating the combination of these EM effects. It is very unlikely, given the size of the ρ region contribution to $a_\mu^{\text{LO,HVP}}$, that this combined EM contribution can be safely neglected. Data-driven results for the subset of EM contributions that can be reliably estimated do, however, provide some useful information which we discuss briefly in the Appendix. We note finally that, although currently unavoidable, the introduction of lattice EM input into an otherwise purely dispersive determination of $a_\mu^{\text{lqc;IL}}$ represents a rather minor "deviation," since the lattice result for the EM correction is, in fact, rather small.

The separation of the IB sum of EM and SIB contributions into separate EM and SIB parts is, as is well known, ambiguous at $O(\alpha_{\text{EM}}(m_d + m_u))$.[5] The separation scheme used by BMW [50] in determining the EM corrections we employ below is defined such that the EM contributions to the masses of the purely connected neutral pseudoscalar mesons are zero, i.e., such that all such EM contributions are absorbed into the definitions of the quark masses. It is numerically very similar to the widely used GRS scheme [82]. By using BMW EM results, we are working in the BMW separation scheme.[6]

To perform the desired EM and SIB corrections, one needs to identify and subtract EM and SIB contributions present in the experimental versions of the nominal $I = 1$ contribution $a_\mu^{I=1}$ determined in the previous section. These

[3]The DV contributions to $a_\mu^{I=1}$ here lie between $-0.34(16) \times 10^{-10}$ and $-0.04(16) \times 10^{-10}$, covering the range from -0.50×10^{-10} to 0.12×10^{-10}. The central value and error of the result quoted in Eq. (3.18) represent, respectively, the midpoint and half the extent of this range.

[4]See, e.g., the discussion of Sec. 2.2.6 of Ref. [3], and Figs. 20 and 22 therein.

[5]For an expanded discussion, see, e.g., Secs. 3.1.1 and 3.1.2 of Ref. [81].

[6]This is, for our purposes, a somewhat academic point since $m_d + m_u$ is only a factor of ∼3 greater than $m_d - m_u$, making the $O(\alpha_{\text{EM}}(m_d + m_u))$ separation ambiguity comparable in size to contributions of $O(\alpha_{\text{EM}}(m_d - m_u))$ which, being second order in IB, we are neglecting throughout.

are of two types: those present in the physical $a_\mu^{I=1}$ contribution itself, and those associated with nominally G-parity positive contributions which are actually part of the mixed-isospin contribution, $a_\mu^{\rm MI}$, and which hence "contaminate" the nominal $a_\mu^{I=1}$ results obtained above. The correction for the mixed-isospin contamination cannot be done inclusively since $\rho_{\rm EM}^{\rm MI}(s)$ receives contributions from both nominally G-parity positive and nominally G-parity negative exclusive modes, with, e.g., $\rho-\omega$ mixing inducing both mixed-isospin $\pi^+\pi^-$ and mixed-isospin $\pi^+\pi^-\pi^0$ contributions, via, respectively, the processes $e^+e^-\to\omega\to\rho\to\pi^+\pi^-$ and $e^+e^-\to\rho\to\omega\to\pi^+\pi^-\pi^0$.

To first order in IB, SIB contributions to $\hat\Pi_{\rm EM}(Q^2)$ and $\rho_{\rm EM}(s)$ occur only in the mixed-isospin parts, while EM contributions are present in all of the $I=1$, $I=0$ and mixed-isospin components. It follows that, to this order, the correction required to convert the physical version of $a_\mu^{33}=a_\mu^{I=1}$ to the corresponding isospin-limit version is purely EM in nature. We denote the associated contribution to $a_\mu^{\rm lqc}$, to be subtracted from the nominal $a_\mu^{\rm lqc}$ obtained in the previous section, by $\delta_{\rm EM}a_\mu^{\rm lqc}$. There is no need for a breakdown of this correction into components associated with individual exclusive modes, and we take as input for this contribution the inclusive lattice result quoted in Ref. [50],

$$\delta_{\rm EM}a_\mu^{\rm lqc}=-0.93(34)(47)\times10^{-10}, \tag{4.1}$$

where the first error is statistical and the second systematic. As noted above, the associated correction represents a very small fraction of the nominal $a_\mu^{\rm lqc}$ results above.

We now address the mixed-isospin-contamination correction. Evaluating this correction requires identifying and subtracting mixed-isospin contaminations present in each of the individual exclusive-mode contributions summed to obtain the nominal $a_\mu^{\rm lqc}$ results of the previous section. In contrast to $a_\mu^{I=1}$, which, to first order in IB, receives no SIB contribution, both EM and SIB contributions are present in $a_\mu^{\rm MI}$, with SIB expected to dominate. In what follows, we rely on experimental input to quantify what should be the dominant exclusive-mode correction and provide conservative bounds on the remaining subdominant contributions. In relying on experimental input, the results for the mixed-isospin corrections are, of course, those for the sum of EM and SIB effects.

As is well known, the strong low-s enhancement produced by the dispersive weight $\hat K(s)/s^2$ is such that the dispersive determination of $a_\mu^{\rm LO,HVP}$ is dominated by contributions from the region of the lowest-lying (especially ρ and ω) resonances. A similar low-s, resonance-region dominance is expected for $a_\mu^{\rm MI}$, doubly so since IB contributions in this region are subject to enhancements generated by the impact of the very small $\rho-\omega$ mass difference on contributions induced by $\rho-\omega$ mixing. In this region, the mixed-isospin spectral contribution, $\rho_{\rm EM}^{\rm MI}(s)$, will appear essentially entirely in the 2π and 3π exclusive modes. Prior to implementing the mixed-isospin correction, the IB 2π and 3π components appear, respectively, in the nominal $I=1$ and $I=0$ sums, and hence represent mixed-isospin contaminations of those sums. In this study, we are interested only in carrying out the mixed-isospin correction for the nominal $I=1$ sum, and hence focus on the IB contribution to the 2π distribution. Note that more than 90% of the full exclusive-mode-region contribution to $a_\mu^{\rm lqc}$, in fact, comes from $\pi\pi$ contributions in the region below $s=1$ GeV^2.

The presence of the obvious $\rho-\omega$ interference "shoulder" in the $e^+e^-\to\pi^+\pi^-$ cross section makes possible an experimental determination of the IB $\rho-\omega$-region contribution from the $\pi\pi$ exclusive-mode. To first order in IB, the associated low-s ($s<1$ GeV^2) contribution to $a_\mu^{\rm LO,HVP}$ lies entirely in $a_\mu^{\rm MI}$. This contribution, which should strongly dominate $[a_\mu^{\rm MI}]_{\pi\pi}$, has recently been determined using the results of a fit to the $e^+e^-\to\pi^+\pi^-$ cross sections based on a dispersively constrained representation of the timelike π form factor incorporating the IB $\rho-\omega$ interference effect [64]. The use of rigorous dispersive constraints turns out to produce a rather tightly constrained result,

$$[a_\mu^{\rm MI}]_{\pi\pi}=3.68(14)(10)\times10^{-10}, \tag{4.2}$$

where the first error is the fit uncertainty and the second the combination of systematic uncertainties. The associated mixed-isospin $\pi\pi$ contamination of the nominal $a_\mu^{\rm lqc}$ obtained in the last section, which we denote $[\delta_{\rm MI}a_\mu^{\rm lqc}]_{\pi\pi}$, is thus

$$[\delta_{\rm MI}a_\mu^{\rm lqc}]_{\pi\pi}=4.09(16)(11)\times10^{-10}. \tag{4.3}$$

This contribution must be subtracted from the nominal $a_\mu^{I=1}$ (i.e., $a_\mu^{\rm lqc}$) results of the previous section.

Note that, in spite of the strong, narrow resonance enhancement, the IB contribution in Eq. (4.2) represents only 0.7% of the full exclusive-mode-region $\pi\pi$ contribution $[a_\mu^{\rm LO,HVP}]_{\pi\pi}$. Since contributions to the nominal $a_\mu^{I=1}$ total from exclusive modes other than $\pi\pi$ are dominated by regions in s for which no analogous narrow interfering resonance enhancements are possible, it should be extremely conservative to assume the magnitudes of contributions to $a_\mu^{\rm MI}$ from all non-$\pi\pi$ exclusive modes are also less than ∼1% of the corresponding nominal $a_\mu^{I=1}$ exclusive-region contributions. The non-$\pi\pi$ exclusive-mode-region contributions to the nominal $I=1$ sum $a_\mu^{I=1}$ total 41.6×10^{-10} in the KNT19 case and 36.7×10^{-10} in the DHMZ case. We thus expect the sum of exclusive-mode-region

contributions to $a_\mu^{\rm MI}$ from all exclusive modes in that sum other than $\pi\pi$ to be less than 0.42×10^{-10} and 0.38×10^{-10} in magnitude, respectively, for the KNT19 case and DHMZ cases. Unsurprisingly, these bounds are much smaller than the accurately determined $\pi\pi$ contribution given in Eq. (4.2). We thus take, as our estimate of the full mixed-isospin contamination present in the nominal $a_\mu^{I=1}$ sums of the previous section, the result of Eq. (4.2), adding the non-$\pi\pi$ exclusive-mode bounds as additional systematic uncertainties.

Adding the results of Eqs. (4.1) and (4.3), we find, for the sum of EM + SIB contributions, $\delta_{\rm EM+SIB}a_\mu^{\rm lqc} \equiv \delta_{\rm EM}a_\mu^{\rm lqc} + [\delta_{\rm MI}a_\mu^{\rm lqc}]_{\pi\pi}$, to be subtracted from the nominal light-quark-connected results, Eqs. (3.11) and (3.21), to convert to the corresponding isospin-limit values, $a_\mu^{\rm lqc;IL}$, the results $\delta_{\rm EM+SIB}a_\mu^{\rm lqc} = 3.16(37)(48)(46) \times 10^{-10}$ and $3.16(37)(48)(41) \times 10^{-10}$ for the KNT19 and DHMZ cases, respectively, where the first errors are statistical, the second are systematic, and the third are the uncertainties estimated above for missing mixed-isospin contributions from non-$\pi\pi$ exclusive modes. Combining, for simplicity of presentation, all errors in quadrature, we obtain the following final results for $a_\mu^{\rm lqc,IL}$:

$$a_\mu^{\rm lqc;IL} = 635.0(2.7) \times 10^{-10} \quad \text{(KNT19)} \qquad (4.4)$$

$$a_\mu^{\rm lqc;IL} = 638.1(4.1) \times 10^{-10} \quad \text{(DHMZ)}. \qquad (4.5)$$

V. CONCLUSIONS AND DISCUSSION

We have shown how recent dispersive results for exclusive-mode contributions to $a_\mu^{\rm LO,HVP}$ can be used to provide a determination of the corresponding isospin-limit, light-quark-connected contribution, $a_\mu^{\rm lqc;IL}$, the precision of which turns out to be of order 0.5%. The determination employs lattice input for a small, 0.15%, EM correction, but is otherwise purely dispersive. The result, of course, depends on the choice of exclusive-mode input, and small differences in the KNT19 and DHMZ assessments of individual exclusive-mode contributions lead to an associated ~0.5% difference between the $a_\mu^{\rm lqc;IL}$ results obtained using KNT19 and DHMZ input, given in Eqs. (4.4) and (4.5), respectively. This difference is similar in size to the errors on the individual KNT19- and DHMZ-based determinations, and sufficiently small to allow meaningful conclusions to be drawn from a comparison of our dispersive results to those of recent lattice analyses. This comparison is summarized in Table I and Fig. 1. Our dispersive results lie lower than the majority of central lattice values, though some variability, at the roughly 2σ level, remains in the lattice results. Among the lattice results, that of Ref. [50] (BMW 2020) has, at present, by far the smallest error, and would strongly dominate any putative lattice average. Our KNT19- and DHMZ-based dispersive results are in 3.2 and 2.4σ tension, respectively, with the BMW 2020 result. Other lattice results, from multiple groups, with similar or smaller errors, are anticipated in the near future, and our dispersive results provide a useful comparison target for such future lattice determinations.

TABLE I. Comparison of our dispersive results with recent lattice results for $a_\mu^{\rm lqc;IL}$. The latter are listed above the internal horizontal line, the former below it.

$a_\mu^{\rm lqc;IL} \times 10^{10}$	Reference
647.6(19.3)	BMW [38]
649.7(15.0)	RBC/UKQCD [40]
629.1(13.7)	ETMC [41,49]
673(14)	PACS [45]
637.8(8.8)	FHM [46]
674(13)	Mainz [47]
659(22)	ABGP [48]
654.5(5.5)	BMW [50]
657(29)	LM [51]
646(14)	ABGP [56]
635.0(2.7)	This work (KNT19-based)
638.1(4.0)	This work (DHMZ-based)

The analysis strategy employed above, though applied there only to the dispersive determination of $a_\mu^{\rm lqc;IL}$, is readily adapted to determinations of other quantities of interest also having a dispersive representation. One well-known example is the standard intermediate window quantity, a_μ^W, introduced by RBC/UKQCD [40], and constructed, by design, to be rather precisely determinable on the lattice. The isospin-limit, light-quark-connected component of a_μ^W, $a_\mu^{\rm W,lqc;IL}$, has now been determined by

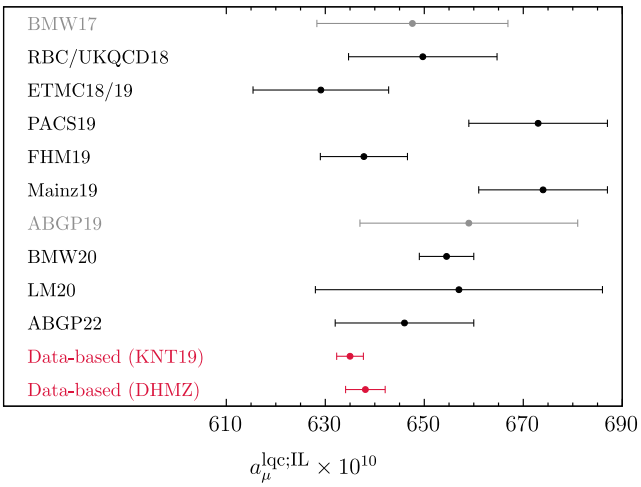

FIG. 1. Comparison of lattice determinations and our dispersive results for $a_\mu^{\rm lqc,IL}$. Lattice results superseded by those from later publications by the same collaboration are plotted in gray. See Table I for the corresponding numerical values and references.

a number of lattice groups [40,48,50,51,53,55–58,60,61], with updates of earlier ABGP [48], ETMc [53] and RBC/UKQCD [40] results, reported in Refs. [56,58,60], bringing results from all groups into excellent agreement. These results are also found to lie significantly higher than alternate mixed "R-ratio + lattice" estimates obtained by subtracting from R-ratio-based dispersive determinations of a_μ^W contributions for all non-light-quark-connected components evaluated on the lattice. Of course, in view of other signs of tension between lattice and dispersive results, one would prefer to compare the rather precise lattice results with a dispersive, rather than mixed lattice-dispersive expectation. This is not currently possible because no purely dispersive $a_\mu^{\mathrm{W,lqc;IL}}$ determination exists.

Weighted exclusive-mode and inclusive-region integrals are, however, equally easy to evaluate for any dispersive weight as they are for the weight $\hat{K}(s)/s^2$ which enters the determinations of the exclusive-mode $a_\mu^{\mathrm{LO,HVP}}$ contributions of Refs. [10,11], provided, that is, the relevant exclusive-mode distributions, $[\rho_{\mathrm{EM}}(s)]_X$, required to perform these reweighted integrals, are publicly available. This information *is* available for the distributions underlying the KNT19 exclusive-mode results of Ref. [11], and KNT19-based dispersive determinations of, not just $a_\mu^{\mathrm{W,lqc;IL}}$, but also other dispersive integral quantities, involving different dispersive weights, are thus also possible using the analysis strategy above.

Quantities of this type likely to be of interest for future investigation include both those naturally formulated in terms of their Euclidean-time (t) weightings and those naturally formulated in terms of their dispersive s-weightings. Examples of the former include the additional intermediate window quantities of Ref. [40], the one-sided window quantities of Ref. [59], the linear-combinations-of-Euclidean-window quantities of Ref. [62], and the window quantity, a_μ^{W2}, introduced in Ref. [56], designed to more strongly weight higher-t lattice contributions and improve the reliability of ChPT-based estimates of lattice finite-volume effects. Examples of the latter are dispersive integrals involving s-dependent weights of the type introduced in Ref. [66], designed to emphasize contributions from more limited regions in s and potentially help in obtaining a more detailed understanding of the source of the current dispersive-lattice tensions. Since the sum of isospin-limit strange-quark-connected and full-disconnected contributions to $\rho_{\mathrm{EM}}(s)$ also has a representation as an appropriately weighted difference of nominally $I = 0$ and nominally $I = 1$ exclusive-mode contributions [65], the current analysis strategy can be employed to determine isospin-limit versions of not just light-quark-connected, but also strange-connected-plus-full-disconnected, contributions to all such window quantities. We plan to implement such dispersive determinations of these various window quantities and will report on the results of this work in a future paper.

ACKNOWLEDGMENTS

This material is based upon work supported by the U.S. Department of Energy, Office of Science, Office of Basic Energy Sciences Energy Frontier Research Centers program under Award No. DE-SC-0013682. D. B.'s work was supported by the São Paulo Research Foundation (FAPESP) Grant No. 2021/06756-6 and by CNPq Grant No. 308979/2021-4. The work of K. M. is supported by a grant from the Natural Sciences and Engineering Research Council of Canada. S. P. is supported by the Spanish Ministry of Science, Innovation and Universities (Project No. PID2020–112965GB-I00/AEI/10.13039/501100011033) and by Grant No. 2017 SGR 1069. I. F. A. E. is partially funded by the CERCA program of the Generalitat de Catalunya.

APPENDIX: IMPLICATIONS OF RECENT RESULTS FOR EM CONTRIBUTIONS FOR WHICH DATA-DRIVEN DETERMINATIONS CURRENTLY EXIST

While at present no data-driven methods are known for determining all EM contributions to $a_\mu^{\mathrm{LO,HVP}}$, the physics underlying a number of such contributions *is* well understood, making reliable, data-driven determinations possible. Several such EM (and/or SIB) contributions are, in addition, numerically enhanced, again for well understood reasons. The question of whether such enhanced IB effects might account for some of the current tension between lattice and data-driven determinations of $a_\mu^{\mathrm{LO,HVP}}$ was recently addressed in Ref. [79], which reviewed results for a set of IB contributions for which improved data-driven determinations are currently available.[7] The results for these contributions, detailed in Ref. [79], are reproduced in Table II. All entries are in units of 10^{-10}.

The first row of the table lists the IB contribution resulting from the impact of the $\pi^\pm - \pi^0$ mass difference on the $a_\mu^{\mathrm{LO,HVP}}$-kernel-enhanced near-threshold-region $\pi\pi$ contribution. Since the pion mass difference is essentially entirely EM in origin, this is, to a good approximation, also a purely EM effect. It results from the fact that the physical $\pi\pi$ threshold, $s = 4m_{\pi^\pm}^2$, lies higher than it would in the isospin limit (where, in the usual definition of the isospin limit, the threshold would be $s = 4m_{\pi^0}^2$). This effect makes the near-threshold $\pi\pi$ contribution larger in the isospin limit. The effect is magnified by the form of the $a_\mu^{\mathrm{LO,HVP}}$ kernel, which strongly enhances contributions from the low-s $\pi\pi$ threshold region. The negative sign of the result reflects the fact that the IB contributions tabulated in Ref. [79] are those contained in the physical result, with

[7]The EM/SIB separation convention implicit in Ref. [79] (that in which the EM π^0 and K^0 self-energies are zero) is, as the authors themselves note, close to the convention employed in recent lattice analyses.

TABLE II. Data-driven results from Ref. [79] for various EM and SIB contributions to $a_\mu^{\mathrm{LO,HVP}}$, in units of 10^{-10}.

Source	EM	SIB
m_{π^+} vs. m_{π^0} kinematic ($\pi\pi$)	−7.67(22)	···
Kaon mass kinematic (K^+K^-)	−3.24(17)	4.98(26)
Kaon mass kinematic ($K^0\bar{K}^0$)	−0.02(0)	−4.62(23)
FSR ($\pi\pi$)	4.42(4)	···
FSR (K^+K^-)	0.75(4)	···
$\rho-\omega$ mixing	···	3.68(17)
$\pi^0\gamma$	4.38(6)	···
$\eta\gamma$	0.70(2)	···
Totals	−0.68(29)	4.04(39)

the isospin limit defined such that the isospin-limit value of the pion mass is m_{π^0}.

The second and third rows of the table give the analogous effects of the EM and SIB contributions to the $K^\pm$ and K^0 masses, the kinematic effects of which are enhanced by the proximity of the physical K^+K^- and $K^0\bar{K}^0$ thresholds to the large ϕ peak in the $e^+e^-\to K\bar{K}$ cross-sections. The signs again reflect the fact that the table entries represent the IB contributions present in the physical result, with the corresponding isospin limit defined as noted above.

The fourth row of the table contains the sum of contributions associated with $\pi\pi$ final state radiation (FSR). This sum is strongly dominated by the $4.24(2)\times 10^{-10}$ $\pi^+\pi^-$ Born-term contribution [79], which is, in turn, dominated by the near-threshold region. The remainder of the quoted total comes from dispersive evaluations [83] of subleading non-Born $\pi^+\pi^-\gamma$ and $\pi^0\pi^0\gamma$ contributions, which contribute 0.15×10^{-10} and 0.03×10^{-10}, respectively. The fifth line of the table gives the analogous K^+K^- FSR contribution.

The sixth row of the table gives the result of the dispersive analysis of Ref. [64] for the IB $\pi\pi$ contribution induced by $\rho-\omega$ mixing. This is "booked" in Ref. [79] as a purely SIB effect, though with a caveat acknowledging the difficulty of reliably breaking down the combined experimental effect into its EM and SIB components at present.

Finally, the seventh and eighth rows of the table give the contributions to $a_\mu^{\mathrm{LO,HVP}}$ associated with the exclusive $\pi^0\gamma$ and $\eta\gamma$ final states. These contributions are dominated by the large radiative ω and ϕ decay peaks in the $e^+e^-\to\pi^0\gamma$ and $e^+e^-\to\eta\gamma$ cross sections and would, of course, vanish in the absence of EM. The $\pi^0\gamma$ contribution is numerically enhanced by the sizeable 8.35(27)% $\omega\to\pi^0\gamma$ branching fraction [71]. The $\omega(\to\pi^0\gamma)$ contribution is, of course, not the only exclusive-mode EM contribution enhanced by the sizeable branching fraction for ω decays to $\pi^0\gamma$ and other "nonpurely pionic" (npp) EM-induced modes. Reference [11], for example, lists contributions of $0.88(2)\times 10^{-10}$, $0.13(1)\times 10^{-10}$ and $0.17(3)\times 10^{-10}$ from the $\pi^0\omega(\to\pi^0\gamma)$, $\omega(\to npp)2\pi$ and $\omega(\to npp)3\pi$ exclusive modes. The sum of these contributions, $1.18(4)\times 10^{-10}$, though only ∼27% of the larger of the two radiative-resonance-decay-enhanced contributions listed in the table (that for $\pi^0\gamma$), is ∼69% larger than the other listed ($\eta\gamma$) contribution.

As noted in Ref. [79], there is a very strong cancellation (by more than an order of magnitude relative to the largest of the individual contributions) in the sum of the tabulated EM contributions. This means that nominally subleading contributions for which no current estimates exist, e.g., the contributions from the ρ peak region discussed in the main text above, or those in the 3π channel discussed in footnote 1 of Ref. [79], are of potential numerical relevance if one's goal is to obtain a data-driven determination of the sum of all EM contributions. The sum, $-0.68(29)\times 10^{-10}$, of the data-driven EM contributions tabulated in Ref. [79] should thus not be interpreted as providing a controlled estimate of the full EM contribution, in spite of the compatibility of that sum, within errors, with the BMW lattice result [50], $-1.45(63)\times 10^{-10}$, for the full EM contribution. That compatibility would, in any case, be considerably degraded were one to add the further $1.18(4)\times 10^{-10}$ in additional, well-quantified, radiative-resonance-decay-enhanced contributions noted above to the Ref. [79] data-driven total. That modified data-driven total would, however, be similarly incomplete.

While, for the reasons given above, we conclude that a controlled data-driven estimate of the full EM contibution is not feasible at present, and hence have chosen to rely on the BMW lattice result for the EM total of interest to us, the determinations of the individual data-driven contributions discussed above do provide some useful, highly nontrivial information. In particular, one learns that, in spite of the existence of a number of individual EM contributions considerably larger in magnitude than the BMW lattice EM result, the scale of the BMW result is "natural," in the sense that the cancellations among these numerically enhanced contributions leave an (albeit incomplete) residue comparable in size to the much smaller BMW result. Such a qualitative conclusion is of use while awaiting results for the full EM total from other lattice groups. The level of this cancellation, which is responsible for the potential numerical relevance of nominally subleading contributions for which no data-driven estimates currently exist, also makes clear the advantage of the lattice determination, which automatically includes all contributions, whether amenable to a data-driven estimate or not, subject to standard, controllable lattice statistical and systematic uncertainties.

[1] B. Abi *et al.* (Muon g-2 Collaboration), Measurement of the Positive Muon Anomalous Magnetic Moment to 0.46 ppm, Phys. Rev. Lett. **126**, 141801 (2021).

[2] G. W. Bennett *et al.* (Muon g-2 Collaboration), Final report of the muon E821 anomalous magnetic moment measurement at BNL, Phys. Rev. D **73**, 072003 (2006).

[3] T. Aoyama, N. Asmussen, M. Benayoun, J. Bijnens, T. Blum, M. Bruno, I. Caprini, C. M. Carloni Calame, M. Cè, G. Colangelo *et al.*, The anomalous magnetic moment of the muon in the Standard Model, Phys. Rep. **887**, 1 (2020).

[4] T. Aoyama, M. Hayakawa, T. Kinoshita, and M. Nio, Complete Tenth-Order QED Contribution to the Muon g-2, Phys. Rev. Lett. **109**, 111808 (2012).

[5] T. Aoyama, T. Kinoshita, and M. Nio, Theory of the anomalous magnetic moment of the electron, Atoms **7**, 28 (2019).

[6] A. Czarnecki, W. J. Marciano, and A. Vainshtein, Refinements in electroweak contributions to the muon anomalous magnetic moment, Phys. Rev. D **67**, 073006 (2003); **73**, 119901(E) (2006).

[7] C. Gnendiger, D. Stöckinger, and H. Stöckinger-Kim, The electroweak contributions to $(g-2)_\mu$ after the Higgs boson mass measurement, Phys. Rev. D **88**, 053005 (2013).

[8] M. Davier, A. Höcker, B. Malaescu, and Z. Q. Zhang, Reevaluation of the hadronic vacuum polarisation contributions to the Standard Model predictions of the muon $g-2$ and $\alpha(m_Z^2)$ using newest hadronic cross-section data, Eur. Phys. J. C **77**, 827 (2017).

[9] A. Keshavarzi, D. Nomura, and T. Teubner, Muon $g-2$ and $\alpha(M_Z^2)$: A new data-based analysis, Phys. Rev. D **97**, 114025 (2018).

[10] M. Davier, A. Höcker, B. Malaescu, and Z. Zhang, A new evaluation of the hadronic vacuum polarisation contributions to the muon anomalous magnetic moment and to $\alpha(m_Z^2)$, Eur. Phys. J. C **80**, 241 (2020); **80**, 410(E) (2020).

[11] A. Keshavarzi, D. Nomura, and T. Teubner, $g-2$ of charged leptons, $\alpha(M_Z^2)$, and the hyperfine splitting of muonium, Phys. Rev. D **101**, 014029 (2020).

[12] G. Colangelo, M. Hoferichter, and P. Stoffer, Two-pion contribution to hadronic vacuum polarization, J. High Energy Phys. 02 (2019) 006.

[13] M. Hoferichter, B.-L. Hoid, and B. Kubis, Three-pion contribution to hadronic vacuum polarization, J. High Energy Phys. 08 (2019) 137.

[14] B.-L. Hoid, M. Hoferichter, and B. Kubis, Hadronic vacuum polarization and vector-meson resonance parameters from $e^+e^- \to \pi^0\gamma$, Eur. Phys. J. C **80**, 988 (2020).

[15] A. Kurz, T. Liu, P. Marquard, and M. Steinhauser, Hadronic contribution to the muon anomalous magnetic moment to next-to-next-to-leading order, Phys. Lett. B **734**, 144 (2014).

[16] K. Melnikov and A. Vainshtein, Hadronic light-by-light scattering contribution to the muon anomalous magnetic moment revisited, Phys. Rev. D **70**, 113006 (2004).

[17] P. Masjuan and P. Sanchez-Puertas, Pseudoscalar-pole contribution to the $(g_\mu-2)$: A rational approach, Phys. Rev. D **95**, 054026 (2017).

[18] G. Colangelo, M. Hoferichter, M. Procura, and P. Stoffer, Rescattering Effects in the Hadronic-Light-by-Light Contribution to the Anomalous Magnetic Moment of the Muon, Phys. Rev. Lett. **118**, 232001 (2017).

[19] G. Colangelo, M. Hoferichter, M. Procura, and P. Stoffer, Dispersion relation for hadronic light-by-light scattering: Two-pion contributions, J. High Energy Phys. 04 (2017) 161.

[20] M. Hoferichter, B.-L. Hoid, B. Kubis, S. Leupold, and S. P. Schneider, Pion-Pole Contribution to Hadronic Light-by-Light Scattering in the Anomalous Magnetic Moment of the Muon, Phys. Rev. Lett. **121**, 112002 (2018).

[21] M. Hoferichter, B.-L. Hoid, B. Kubis, S. Leopold, and S. P. Schneider, Dispersion relation for hadronic light-by-light scattering: Pion pole, J. High Energy Phys. 10 (2018) 141.

[22] A. Gérardin, H. B. Meyer, and A. Nyffeler, Lattice calculation of the pion transition form factor with $N_f = 2+1$ Wilson quarks, Phys. Rev. D **100**, 034520 (2019).

[23] J. Bijnens, N. Hermansson-Truedsson, and A. Rodriguez-Sanchez, Short-distance constraints for the HLbL contribution to the muon anomalous magnetic moment, Phys. Lett. B **798**, 134994 (2019).

[24] G. Colangelo, F. Hagelstein, M. Hoferichter, L. Laub, and P. Stoffer, Short-distance constraints on hadronic light-by-light scattering in the anomalous magnetic moment of the muon, Phys. Rev. D **101**, 051501 (2020).

[25] G. Colangelo, F. Hagelstein, M. Hoferichter, L. Laub, and P. Stoffer, Longitudinal short-distance constraints for the hadronic light-by-light contribution to $(g-2)_\mu$ with large-N_c Regge models, J. High Energy Phys. 03 (2020) 101.

[26] G. Colangelo, M. Hoferichter, A. Nyffeler, M. Passera, and P. Stoffer, Remarks on higher-order hadronic corrections to the muon $g-2$, Phys. Lett. B **735**, 90 (2014).

[27] T. Blum, N. Christ, M. Hayakawa, T. Izubuchi, L.-C. Jin, C. Jung, and C. Lehner, Hadronic Light-by-Light Scattering Contribution to the Muon Anomalous Magnetic Moment from Lattice QCD, Phys. Rev. Lett. **124**, 132002 (2020).

[28] S. J. Brodsky and E. De Rafael, Suggested boson-lepton pair couplings and the anomalous magnetic moment of the muon, Phys. Rev. **168**, 1620 (1968).

[29] B. E. Lautrup and E. De Rafael, Calculation of the sixth-order contribution from the fourth-order vacuum polarization to the difference of the anomalous magnetic moments of muon and electron, Phys. Rev. **174**, 1835 (1968).

[30] M. Gourdin and E. De Rafael, Hadronic contributions to the muon g-factor, Nucl. Phys. **B10**, 667 (1969).

[31] B. E. Lautrup, A. Peterman, and E. De Rafael, Recent developments in the comparison between theory and experiments in quantum electrodynamics, Phys. Rep. **3**, 193 (1972).

[32] E. De Rafael, Hadronic contributions to the muon g-2 and low-energy QCD, Phys. Lett. B **322**, 239 (1994).

[33] T. Blum, Lattice Calculation of the Lowest Order Hadronic Contribution to the Muon Anomalous Magnetic Moment, Phys. Rev. Lett. **91**, 052001 (2003).

[34] B. Chakraborty, C. T. H. Davies, G. C. Donald, R. J. Dowdall, J. Koponen, G. P. Lepage, and T. Teubner, Strange and charm quark contributions to the anomalous magnetic moment of the muon, Phys. Rev. D **89**, 114501 (2014).

[35] T. Blum, P. A. Boyle, T. Izubuchi, L. Jin, A. Jüttner, C. Lehner, K. Maltman, M. Marinkovic, A. Portelli, and M. Spraggs, Calculation of the Hadronic Vacuum Polarization Disconnected Contribution to the Muon Anomalous Magnetic Moment, Phys. Rev. Lett. **116**, 232002 (2016).

[36] B. Chakraborty, C. T. H. Davies, P. G. Oliviera, J. Koponen, G. P. Lepage, and R. S. Van de Water, The hadronic vacuum polarization contribution to a_μ from full lattice QCD, Phys. Rev. D **96**, 034 (2017).
[37] T. Blum *et al.*, Lattice calculation of the leading strange quark-connected contribution to the muon $g-2$, J. High Energy Phys. 04 (2017) 063; 05 (2017) 034(E).
[38] Sz. Borsanyi *et al.*, Hadronic Vacuum Polarization Contribution to the Anomalous Magnetic Moments of Leptons from First Principles, Phys. Rev. Lett. **121**, 022002 (2018).
[39] D. Giusti, V. Lubicz, G. Martinelli, F. Sanfilippo, and S. Simula, Strange and charm HVP contributions to the muon $(g-2)$ including QED corrections with twisted-mass fermions J. High Energy Phys. 10 (2017) 157.
[40] T. Blum, P. A. Boyle, V. Gülpers, T. Izubuchi, L. Jin, C. Jung, A. Jüttner, C. Lehner, A. Portelli, and J. T. Tsang, Calculation of the Hadronic Vacuum Polarization Contribution to the Muon Anomalous Magnetic Moment, Phys. Rev. Lett. **121**, 022003 (2018).
[41] D. Giusti, F. Sanfilippo, and S. Simula, Light-quark contribution to the leading hadronic vacuum polarization term of the muon $g-2$ from twisted-mass fermions, Phys. Rev. D **98**, 114504 (2018).
[42] D. Giusti, V. Lubicz, G. Martinelli, F. Sanfilippo, S. Simula, and C. Tarantino, HVP contribution of the light quarks to the muon $(g-2)$ including isospin-breaking corrections with twisted-mass fermions, Proc. Sci. LATTICE2018 (**2018**) 140.
[43] V. Gülpers, A. Jüttner, C. Lehner, and A. Portelli, Isospin breaking corrections to the HVP at the physical point, Proc. Sci. LATTICE2018 (**2018**) 134.
[44] D. Giusti, V. Lubicz, G. Marinelli, F. Sanfilippo, and S. Simula, Electromagnetic and strong isospin-breaking corrections to the muon $g-2$ from Lattice QCD + QED, Phys. Rev. D **99**, 114502 (2019).
[45] E. Shintani and Y. Kuramashi, Hadronic vacuum polarization contribution to the muon $g-2$ with $2+1$ flavor lattice QCD on a larger than $(10\ \mathrm{fm})^4$ lattice at the physical point, Phys. Rev. D **100**, 034517 (2019).
[46] C. T. H. Davies *et al.*, Hadronic-vacuum-polarization contribution to the muon's anomalous magnetic moment from four-flavor lattice QCD, Phys. Rev. D **101**, 034512 (2020).
[47] A. Gérardin, M. Cè, G. von Hippel, B. Hörz, H. B. Meyer, D. Mohler, K. Ottnad, J. Wilhelm, and H. Wittig, The leading hadronic contribution to $(g-2)_\mu$ from lattice QCD with $N_\mathrm{f}=2+1$ flavours of $\mathrm{O}(a)$ improved Wilson quarks, Phys. Rev. D **100**, 014510 (2019).
[48] C. Aubin, T. Blum, C. Tu, M. Golterman, C. Jung, and S. Peris, Light quark vacuum polarization at the physical point and contribution to the muon $g-2$, Phys. Rev. D **101**, 014503 (2020).
[49] D. Giusti and S. Simula, Lepton anomalous magnetic moments in Lattice QCD + QED, Proc. Sci. LATTICE2019 (**2019**) 104.
[50] S. Borsanyi, Z. Fodor, J. N. Guenther, C. Hoelbling, S. D. Katz, L. Lellouch, T. Lippert, K. Miura, L. Parato, K. K. Szabo *et al.*, Leading hadronic contribution to the muon magnetic moment from lattice QCD, Nature (London) **593**, 51 (2021).
[51] C. Lehner and A. S. Meyer, Consistency of hadronic vacuum polarization between lattice QCD and the R-ratio, Phys. Rev. D **101**, 074515 (2020).
[52] C. Aubin, T. Blum, M. Golterman, and S. Peris, The muon $g-2$ with four flavors of staggered quarks, Proc. Sci. LATTICE2021 (**2022**) 161.
[53] D. Giusti and S. Simula, Window contributions to the muon hadronic vacuum polarization with twisted-mass fermions, Proc. Sci. LATTICE2021 (**2022**) 189.
[54] A. Risch and H. Wittig, Leading isospin breaking effects in the HVP contribution to a_μ and to the running of α, Proc. Sci. LATTICE2021 (**2022**) 106.
[55] G. Wang, T. Draper, K.-F. Liu, and Y.-B. Yang (chiQCD Collaboration), Muon g-2 with overlap valence fermion, Phys. Rev. D **107**, 034513 (2023).
[56] C. Aubin, T. Blum, M. Golterman, and S. Peris, The muon anomalous magnetic moment with staggered fermions: Is the lattice spacing small enough?, Phys. Rev. D **106**, 054503 (2022).
[57] M. Cè, A. Gérardin, G. von Hippel, R. J. Hudspith, S. Kuberski, H. B. Meyer, K. Miura, D. Mohler, K. Ottnad, S. Paul *et al.* Window observable for the hadronic vacuum polarization contribution to the muon $g-2$ from lattice QCD, Phys. Rev. D **106**, 114502 (2022).
[58] C. Alexandrou, S. Bacchio, P. Dimopoulos, J. Finkenrath, R. Frezzotti, G. Gagliardi, M. Garofalo, K. Hadjiyiannakou, B. Kostrzewa, K. Jansen *et al.*, Lattice calculation of the short and intermediate time-distance hadronic vacuum polarization contributions to the muon magnetic moment using twisted-mass fermions, arXiv:2206.15084.
[59] C. T. H. Davies, C. DeTar, A. X. El-Khadra, S. Gottlieb, D. Hatton, A. S. Kronfeld, S. Lahert, G. P. Lepage, C. McNeile, E. T. Neil *et al.*, Windows on the hadronic vacuum polarization contribution to the muon anomalous magnetic moment, Phys. Rev. D **106**, 074509 (2022).
[60] T. Blum, P. A. Boyle, M. Bruno, D. Giusti, V. Gülpers, R. C. Hill, T. Izubuchi, Y. C. Jang, L. Jin, C. Jung *et al.*, An update of Euclidean windows of the hadronic vacuum polarization, arXiv:2301.08696.
[61] A. Bazavov, C. Davies, C. De Tar, A. X. El-Khadra, E. Gamiz, S. Gottlieb, W. I. Jay, H. Jeong, A. S. Kronfeld, S. Lahert *et al.*, Light-quark connected intermediate-window contributions to the muon $g-2$ hadronic vacuum polarization from lattice QCD, arXiv:2301.08274.
[62] G. Colangelo, A. X. El-Khadra, M. Hoferichter, A. Keshavarzi, C. Lehner, P. Stoffer, and T. Teubner, Data-driven evaluations of Euclidean windows to scrutinize hadronic vacuum polarization, Phys. Lett. B **833**, 137313 (2022).
[63] C. L. James, R. Lewis, and K. Maltman, ChPT estimate of the strong-isospin-breaking contribution to the anomalous magnetic moment of the muon, Phys. Rev. D **105**, 053010 (2022).
[64] G. Colangelo, M. Hoferichter, B. Kubis, and P. Stoffer, Isospin-breaking effects in the two-pion contribution to hadronic vacuum polarization, J. High Energy Phys. 10 (2022) 032.
[65] D. Boito, M. Golterman, K. Maltman, and S. Peris, Evaluation of the three-flavor quark-disconnected contribution to the muon anomalous magnetic moment from experimental data, Phys. Rev. D **105**, 093003 (2022).

[66] D. Boito, M. Golterman, K. Maltman, and S. Peris, Spectral weight sum rules for the hadronic vacuum polarization, Phys. Rev. D **107**, 034512 (2023).
[67] J. P. Lees *et al.* (*BABAR* Collaboration), Measurement of the spectral function for the $\tau^- \to K^- K_S \nu_\tau$ decay, Phys. Rev. D **98**, 032010 (2018).
[68] B. Aubert *et al.* (*BABAR* Collaboration), Measurements of $e^+e^- \to K^+K^-\eta$, $K^+K^-\pi^0$ and $K^0_S K^\pm \pi^\mp$ cross sections using initial state radiation events, Phys. Rev. D **77**, 092002 (2008).
[69] P. A. Baikov, K. G. Chetyrkin, and J. H. Kuhn, Order α_s^4 QCD Corrections to Z and τ Decays, Phys. Rev. Lett. **101**, 012002 (2008).
[70] F. Herzog, B. Ruijl, T. Ueda, J. A. M. Vermaseren, and A. Vogt, The five-loop beta function of Yang-Mills theory with fermions, J. High Energy Phys. 02 (2017) 090.
[71] P. A. Zyla *et al.* (Particle Data Group), Review of particle properties, Prog. Theor. Exp. Phys. **2020**, 083C01 (2020).
[72] J. Z. Bai *et al.* (BES Collaboration), Measurements of the Cross-Section for $e^+e^- \to$ Hadrons at Center-of-Mass Energies from 2 GeV to 5 GeV, Phys. Rev. Lett. **88**, 101802 (2002).
[73] M. Ablikim *et al.* (BES Collaboration), R value measurements for e^+e^- annihilation at 2.60 GeV, 3.07 GeV and 3.65 GeV, Phys. Lett. B **677**, 239 (2009).
[74] V. V. Anashin *et al.* (KEDR Collaboration), Precise measurement of $R_{\rm uds}$ and R between 1.84 and 3.72 GeV at the KEDR detector, Phys. Lett. B **788**, 42 (2019).
[75] M. Ablikim *et al.* (BESIII Collaboration), Measurement of the Cross Section for $e^+e^- \to$ Hadrons at Energies from 2.2324 to 3.6710 GeV, Phys. Rev. Lett. **128**, 062004 (2022).
[76] D. Boito, M. Golterman, K. Maltman, S. Peris, M. V. Rodrigues, and W. Schaaf, Strong coupling from an improved τ vector isovector spectral function, Phys. Rev. D **103**, 034028 (2021).
[77] D. Boito, I. Caprini, M. Golterman, K. Maltman, and S. Peris, Hyperasymptotics and quark-hadron duality violations in QCD, Phys. Rev. D **97**, 054007 (2018).
[78] J. P. Lees *et al.* (*BABAR* Collaboration), Cross sections for the reactions $e^+e^- \to K^+K^-\pi^+\pi^-$, $K^+K^-\pi^0\pi^0$, and $K^+K^-K^+K^-$ measured using initial-state radiation events, Phys. Rev. D **86**, 012008 (2012).
[79] M. Hoferichter, G. Colangelo, B.-L. Hoid, B. Kubis, J. R. de Elvira, D. Stamen, and P. Stoffer, Chiral extrapolation of hadronic vacuum polarization and isospin-breaking corrections, Proc. Sci. LATTICE2022 (**2022**) 316.
[80] J. Bijnens and P. Gosdzinsky, Electromagnetic contributions to vector meson masses and mixings, Phys. Lett. B **388**, 203 (1996).
[81] S. Aoki *et al.* (Flavor Lattice Averaging Group), FLAG review 2019: Flavour Lattice Averaging Group (FLAG), Eur. Phys. J. C **80**, 113 (2020).
[82] J. Gasser, A. Rusetsky, and I. Scimemi, Electromagnetic corrections in hadronic processes, Eur. Phys. J. C **32**, 97 (2003).
[83] B. Moussallam, Unified dispersive approach to real and virtual photon-photon scattering at low energy, Eur. Phys. J. C **73**, 2539 (2013).